Volume 3 | Number 44 | 28 November 2015 | Pages 11557–11774

Journal of Materials Chemistry C

Materials for optical, magnetic and electronic devices

www.rsc.org/MaterialsC

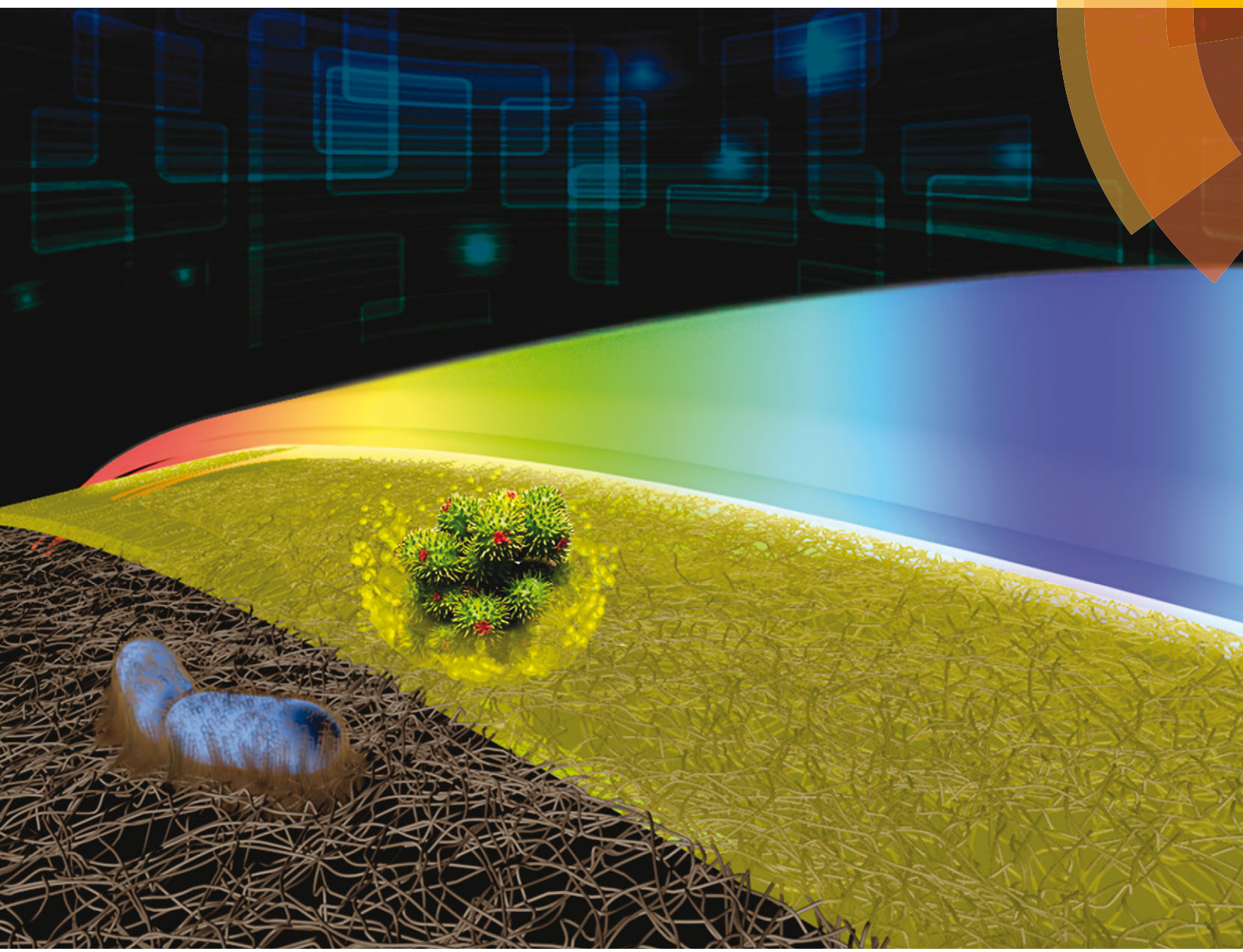

ISSN 2050-7526

ROYAL SOCIETY OF CHEMISTRY

PAPER

H. S. Barud *et al.*

Transparent composites prepared from bacterial cellulose and castor oil based polyurethane as substrates for flexible OLEDs

Journal of Materials Chemistry C

PAPER

View Article Online
View Journal | View Issue

Cite this: J. Mater. Chem. C, 2015, 3, 11581

Transparent composites prepared from bacterial cellulose and castor oil based polyurethane as substrates for flexible OLEDs

E. R. P. Pinto,†[a] H. S. Barud,†*[ab] R. R. Silva,[a] M. Palmieri,[a] W. L. Polito,[c] V. L. Calil,[c] M. Cremona,[d] S. J. L. Ribeiro[a] and Y. Messaddeq[a]

Received 30th July 2015,
Accepted 18th September 2015

DOI: 10.1039/c5tc02359a

www.rsc.org/MaterialsC

Flexible and transparent composites were prepared from bacterial cellulose (BC) and castor oil based polyurethane (PU). The new BC/PU composites exhibit excellent transparency (up to 90%) in the visible region and great mechanical properties, with a tensile strength of up to 69 MPa and a Young's Modulus up to 6 GPa. The resulting free-standing thin films possessed low surface roughness (below 1 nm), and whose properties suggest a potential candidate substrate for flexible light emitting devices. Subsequently, the fabrication of flexible organic light emitting diodes (flexible OLEDs) was successfully investigated by using flexible transparent BC/PU membranes rather than standard flat glass substrates.

Introduction

Bacterial cellulose (BC) membranes are produced by some bacteria such as the species *Gluconacetobacter xylinus*.[1] Essentially, BC is a hydrogel formed of 1 wt% of an interesting 3D network of fibers with diameters below 100 nm (nanoscale range). Unlike plant-based cellulose fibers, BC nanofibers have many unique properties including a high degree of polymerization and crystallinity besides higher tensile strength (200–300 MPa) and Young's modulus (up to 78 GPa) which make them 8 times stronger than stainless steel.[2] These particular features introduce BC membranes into a wealth of applications, such as reinforcing agents for composites throughout substrates of highly desired optical materials.[3] In fact, BC nanofibers are very strong but also very lightweight. Because of the small lateral dimensions of individual BC nanofibers, they display negligible light scattering and as a result their particularly rich and exciting physics come into play, making them attractive materials for the reinforcement of transparent substrates for electronic displays.

At present, organic light emitting diodes (OLEDs) are traditionally fabricated on rigid glass sheet substrates.[4] However, flexible polymer substrates have been explored as a potential alternative in replacing glass substrates.[5–7] An additional and highly desirable feature is the use of a high content of biopolymers in the manufacture of flexible substrates. Owing to their inherent nature, BC nanofibers possess high tensile strength, a low coefficient of thermal expansion (*i.e.* 0.1 ppm K^{-1})[8] besides exceptional flexibility which introduce significant improvements of the mechanical properties of derived composites.

Much work has been focused on the pursuit of the rational design of BC composite materials with relevant optical and mechanical properties and commercially comparable to current engineered plastics.[5,7,9] An increasing number of approaches have explored the fabrication of transparent nanobiocomposites based on BC and renewable biopolymer sources. Some of these nanobiocomposites include BC/chitosan,[10] BC/polyhydroxybutirate,[11] BC/polyvinyl alcohol,[12] BC/boehmite-epoxi-siloxane,[13] BC/poly-(L-lactic acid),[14] among others. Nevertheless, work has also been dedicated to the fabrication of highly transparent BC composites based on impregnation with resins. Yano *et al.*[15] developed highly transparent composites based on BC membranes impregnated with epoxy, acrylic and phenol-formaldehyde resins. In general, the composites display a high fiber content (70 wt%) with outstanding mechanical strength and low thermal expansion coefficients.[15]

Among various resins from renewable resources,[16] polyurethane (PU) is a versatile polymer produced from different raw materials and widely used in several applications such as hard and flexible foams, thermoplastics, thermosetting, coatings, elastomers and adhesives. The main advantage of PU resins is their segmented domain structure, which can be tailored over a considerable range through the selection of the raw materials, their relative proportions, and the processing conditions. Vegetable oils such as canola oil, corn oil, linseed oil, palm oil, soybean oil and

[a] Institute of Chemistry – São Paulo State University – UNESP, Araraquara, São Paulo 14801-970, Brazil. E-mail: hernane.barud@gmail.com
[b] Centro universitário de Araraquara – UNIARA, Araraquara, São Paulo 14801-320, Brazil
[c] Institute of Chemistry – São Paulo University – USP, São Carlos, São Paulo 13560-250, Brazil
[d] Department of Physics – Pontifical Catholic University – PUC, Rio de Janeiro 22451-900, Brazil
† These authors contributed equally to this work.

sunflower oil have been explored as raw sources in the manufacture of PU resins.[17] Of note, castor oil is one the most investigated natural oil polyols used to prepare PU. Castor oil is majority composed (*i.e.* 90%) of the tri-esters of rincinoleic acid and glycerin, which result in an interesting precursor rich in groups such as hydroxyl groups and carbon–carbon double bonds.[18–20]

PU resin can be synthesized as a chemically active prepolymer. Essentially, the PU prepolymer has free isocyanate groups, which in turn easily bind with hydroxyl groups to produce urethane bonds. In this sense, it is feasible and even predictable that a PU prepolymer may have the ability to fashion a strong interface with the hydroxyl groups present on the surface of BC nanofibers through urethane bonds. Indeed, there has been work that has investigated the use of plant cellulose[22–25] or lignin[21] and PU resin to produce improved composites. To date, Manuspiya *et al.*[26,27] have exploited the design of film composites based on the impregnation of commercial PU resin into dried BC membranes (10–50%) for flexible OLEDs. The BC-derived films were found to have a reduced water absorption after the impregnation of PU besides remarkable flexibility and transparency (>80% at 550 nm).[27] It should be pointed out that most of the work relies on PU derived from petrochemical resources.[28,29]

Herein, transparent and bendable nanocomposites with high bio-content were prepared by the impregnation of a PU prepolymer derived from castor oil into dried BC membranes. The BC/PU composites displayed a high BC fiber content (up to 70%), low roughness, high thermal stability, and excellent mechanical properties. Flexible OLEDs based on the BC/PU membranes were fashioned and their electric and optical properties were evaluated.

Experimental

Materials

Refined castor oil, first special grade (FSG) was produced from a local oil company, Aboissa. Trimethylolpropane, propylene glycol, xylene, ethyl glycol acetate and ethanol puriss. p.a. were all purchased from Sigma Aldrich. Toluene–diisocyanate 80/20 (TDI) was purchased from Brazmo. (2-Phenylpyridine)iridium(III) ($Ir(ppy)_3$), copper phthalocyanine (CuPc, 99%), *N*,*N*′-bis(1-naphthyl)-*N*,*N*′-diphenyl-1,1′-biphenyl-4,4′-diamine (NPB), 4,4′-bis(carbazol-9-yl)biphenyl (CBP), 2,9-dimethyl-4,7-diphenyl-1,10-phenanthroline (BCP), tris(8-hydroxyquinoline) aluminum (Alq_3) and aluminum (Al) were all purchased from LumTec Corp. SiO_2 and ceramic $In_2O_3:SnO_2$ (90 : 10 wt%, 99.99% purity) targets were purchased from Kurt J. Lesker.

Culture media for the production of membranes of bacterial cellulose

Never-dried BC membranes (5 × 6 cm, 5 mm thick) were produced from an isolated culture of a wild strain of *Gluconacetobacter xylinus* (American Type Culture Collection, ATCC 23769). A cultivation medium was conducted at 28 °C for 96 h in trays with dimensions of 30 cm × 50 cm, containing a sterile medium composed of 50 g L^{-1} glucose, 4 g L^{-1} yeast extracts, 2 g L^{-1} anhydrous disodium phosphate, 0.8 g L^{-1} heptahydrated magnesium sulphate, and 20 g L^{-1} ethanol. After 96 h, the hydrated BC hydrogel membranes were about 3 mm thick. The BC membranes were composed of 1 wt% cellulose and 99 wt% water. The membranes were washed several times under water flux. An aqueous solution of 1 wt% NaOH at 70 °C was added in order to remove the remaining bacteria and water until a neutral pH was achieved. Dried BC membranes were obtained by drying hydrated membranes at 80 °C between two Teflon plates.

Synthesis of the castor oil based polyurethane prepolymer

The polyurethane prepolymer (PU) was synthesized with TDI and a polyol consisting of castor oil as the main component. The synthesis of the PU prepolymer was performed in a stainless steel reactor (1 kg capacity) at ambient pressure (1 atm). The molar ratio between the isocyanate and hydroxyl groups was set at 1.1–1.0 and the prepolymer had 4% of free isocyanate. The synthesis of the PU prepolymer was reported by De Carlo (2002),[30] which used the following components: castor oil (OH = 180 mg KOH g^{-1} sample), trimethylolpropane, propylene(glycol), TDI, xylene and ethyl glycol acetate. The polymerization reaction was placed in a reactor where the components were added with one shot. The reaction was conducted for 8 h at 85 °C under a nitrogen atmosphere and with vigorous agitation.

Preparation of the flexible transparent BC/PU composites

Dried BC membranes (5 cm × 6 cm, 20 μm thick) were coated with neat PU prepolymer (4 wt% isocyanate-free) on both sides. The membrane was held with a handy rectangular Teflon device with screws at the corners. Therefore, the BC membrane was merged in solvents of different polarity, which in turn were selected according to the low cost of processability and whichever afforded the best interface with the PU prepolymer (*i.e.* prevention of phase separation). (a) The first solvent was ethanol in order to remove any residual water on the surface of the BC nanofibers. Afterwards, ethanol was exchanged by merging the BC membrane in ethyl glycol acetate, a common solvent for the PU prepolymer. Two periods of time were chosen for this study: 72 h and 120 h. The samples were named as BC/PU72 and BC/PU120. (b) The BC membranes were coated with the neat PU prepolymer (4 wt% of free isocyanate) for approximately 5 minutes. (c) The BC/PU composites were dried at ambient temperature for 24 h in a rectangular Teflon device.

Preparation of the flexible transparent BC/PU membrane substrates for flexible OLEDs

The BC/PU composites were coated with SiO_2 and indium tin oxide (ITO) thin films, seeking to increase the electrical conductance of the membrane. The depositions were carried out in an Åmod Series Coating System from Angstrom Engineering, equipped with a 3-inch magnetron gun. A radio frequency power of 13.56 MHz was supplied by an radio frequency generator matched to the target by a tuning network, both from Advanced Energy. SiO_2 and ITO were deposited using 100 W and 80 W power deposition for a final thickness of 100 nm and 300 nm, respectively. A work pressure of 0.27 Pa was applied for both materials.

Flexible OLED devices were fabricated using high vacuum thermal evaporation of the organic materials with the usual $Ir(ppy)_3$ based OLED architecture: CuPc, NPB, a co-deposited layer of CBP as the matrix and $Ir(ppy)_3$ as the dopant, BCP, Alq_3 and Al. The base pressure was 1.0 mPa ($\sim 8 \times 10^{-6}$ Torr) and during evaporation the pressure was between 1.3 mPa and 6.7 mPa. The deposition rates for the organic and Al films were 3 and 18 nm min^{-1}, respectively. In order to compare the flexible OLED performance, a reference device was fabricated using a flat glass slide as the substrate.

Optical and structural properties of BC/PU composites

Transmission spectra were recorded in an ultraviolet-visible-near infrared Varian-CARY 500 spectrophotometer in the 800–300 nm wavelength interval. The refractive index was obtained by using a Metricon mod. 2010 prism coupler equipped with a He–Ne laser operating at 543.5 nm. Scanning electron microscopy (SEM) measurements were performed with a SEM-JEOL 6700F instrument. Samples were covered with a 3 nm thick Pt layer. AFM was performed with an Agilent 5500 SPM AC Mode III instrument (Agilent Technologies) under ambient conditions (22 °C, 45–55% relative humidity) over areas of 5 μm × 5 μm and 1 μm × 1 μm. The instrument was equipped with a silicon (aluminum coating) tip with a resonance frequency of 204–497 KHz and force constant of 10–130 N m^{-1}, operated in tapping mode. The measurements were repeated five times for a comparable topological analysis. Image and roughness analyses were conducted using the Gwyddion 2.31 software.

X-ray diffraction patterns were obtained with a Siemens Kristalloflex diffractometer using nickel filtered Cu Kα radiation, a step size of 0.02° and a step time of 3 s, from 5° to 50° (2θ angle). The mechanical measurements were performed at room temperature with a Dynamic Mechanical Analyzer (DMA) 2980 from TA Instruments, equipped with a film tension clamp. Specimens' dimensions were 1 cm × 0.25 cm. Thickness values varied from 10 μm to 35 μm. A preload force of 0.01 N was used and a force ramp 18 N m^{-1} until the rupture of the sample. The device was previously calibrated and 10 measurements for each sample were obtained to ensure the reproducibility of the results.

Characterization of the BC/PU composite as a substrate for flexible OLEDs

The electrical properties of the functionalized BC/PU composite and glass substrate were measured using a four-point probe technique, in an ECOPIA Hall Effect Measurement System HS 3000. The film thickness was measured using a Dektak6M Stylus Profile from Veeco. The luminance was measured directly using a calibrated Konica Minolta Luminance Meter LS-100. The current–voltage (*I–V*) characteristics were measured with a programmable voltage current source (Keithley 2400).

Results and discussion

The nominal composition and thickness of the resulting flexible and freestanding BC/PU composites are described in the Table 1.

Table 1 Specifications of the composition of the BC/PU composites

	BC (wt%)	PU prepolymer (wt%)	Thickness (μm)
Pristine BC	100	—	20
BC/PU72	79	21	21
BC/PU120	74	26	22
Pure PU film	—	100	15

Pristine dried BC membranes showed usual poor transparency while the BC/PU composites, possessing a high content of cellulose (>70 wt%), exhibited high transparency. Additionally, the BC/PU nanocomposites displayed reliable flexibility and macroscopic homogeneity as highlighted in the pictures in Fig. 1. The transmittance spectra in the ultraviolet-visible region of the pristine dried BC membranes and BC/PU composites dried in different periods of time are shown in Fig. 1A. The blue vector picture behind the bended BC/PU composite was clearly visible in Fig. 1B compared to the translucent pristine BC membrane shown in Fig. 1C. The transmission spectra of the BC/PU composites were carefully evaluated taking into account the eventual disparities of the sheet thickness among the samples.

As expected, the pristine BC membrane displayed very poor transparency in the UV-vis region with transmittance values of 8% at 350 nm and 63% at 700 nm. On the other hand, the BC/PU composites showed a significant increase in transparency with a transmittance larger than 70% at 350 nm. The BC/PU composites showed high transparency in the visible range. For example, BC membranes subjected to 72 h of solvent exchange, BC/PU72, displayed a transparency of 82% at 700 nm whereas BC membranes that were allowed to exchange solvent for an additional 48 h (120 h in total, BC/PU120), exhibited a transparency of 90% at 700 nm. A slight decrease in transparency was found for BC/PU72 once it comprised a composite with more BC nanofiber content, which in turn addresses the additional light scattering.

The significant transparency of the BC/PU composites is conceived by the overlapping of the optical properties of both the pure PU films and the 3D network assembly of the BC nanofibers.

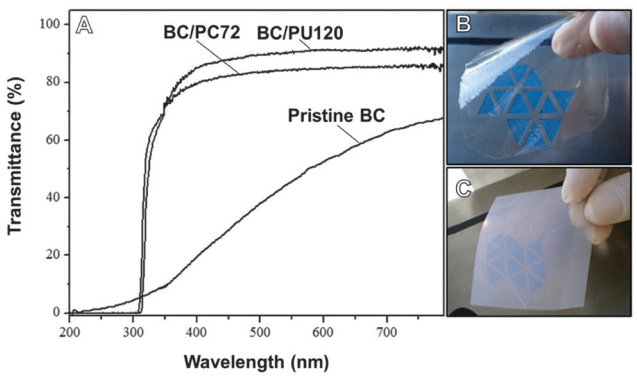

Fig. 1 (A) Transmittance spectra in the ultraviolet-visible wavelength interval of 200–800 nm for the pristine dried BC membrane and BC/PU composite resulted from the solvent exchange processes within 72 h and 120 h. The digital images in (B) and (C) highlight the difference in transparency between the BC/PU composite resulted from the solvent exchange process within 72 h and the dried BC membrane, respectively.

It should be noted that the refractive index (η) is the most striking feature which has to be taken into consideration in the design of composites with enhanced optical qualities. Essentially, the BC membrane presents two η values: 1.618 for the parallel direction toward the crystal axis ($\eta_{\parallel}$) and 1.544 for the perpendicular direction toward the chain orientation ($\eta_{\perp}$).[31] In fact, the contrast between the refractive index of the cellulose fibers ($\eta > 1.5$) and air ($\eta = 1$), existing in the interstices of the dried pristine BC membrane, causes light scattering. However, the BC membrane became very transparent after the introduction of the PU prepolymer. We carried out the measurement of the η value of the pure PU film derived from castor oil and the BC/PU composites using the M-lines technique. In fact, all BC/PU composites exhibited the same η value of 1.544 whereas the pure PU film had a value of 1.526. Therefore, it is suggested that the proximity between the η value of the pure PU film and the $\eta_{\perp}$ value of the BC nanofibers may elucidate the remarkable transparency of the BC membranes coated with PU resin.

Fig. 2A and B show the SEM images of the surface of the pristine dried BC and BC/PU72 composite, respectively. The surface of the dried BC membrane was formed by a compact 3D network of random assemblages of BC nanofibril bundles that clutch into flat ribbon- and filamentary-shaped cellulose fibers with diameters ranging from 50 to 100 nm.[9,15,32] Fig. 2B shows the BC membrane surface when it was totally covered by PU resin. The 3D network of cellulose nanofibers completely disappeared on the surface of the BC/PU composites after impregnation with PU. The cross section image of the BC shown in Fig. 2C reveals unoriented BC nanofibrils organized into plate-like structures loosely spaced from each other. It is worth pointing out that any change of morphology in the BC nanofibers was observed in the nanocomposites. On the other hand, the SEM image of the cross section of the BC/PU72 composite in Fig. 2D shows that the PU resin did not only cover the surface of the BC, but also penetrated through the plate-like structures of the BC. As a result, the air interstices of neat BC were filled with PU resin, which in turn yielded a sheet arranged by tightly compacted layers of BC nanofibers.[26]

The process of solvent exchange (*i.e.* water that was replaced by ethyl glycol acetate) employed in the never-dried BC membranes had a notable role in the fabrication of composites with a very consistent layered structure. We believe that the use of ethyl glycol acetate greatly allowed the penetration of the PU prepolymer in the BC membrane because it was the common solvent in BC and the PU prepolymer. The same behavior was observed by Bismarck *et al.*[33] when never dried BC membranes were subjected to solvent exchange using only ethanol. Hopefully, the present work may contribute meaningful information on the improvement of the penetration of PU prepolymer into BC membranes by a simple solvent exchange approach. The impregnation of PU resin through the BC membrane leads to new urethane bonds as highlighted by the schematic illustration pictured in Fig. 3. The urethane bonds produce a strong interface between the cellulose nanofibers and PU of the composite that interconnect the entire 3D network of BC nanofibers.

Once the network of BC nanofibers were not detected in the SEM of the surface of the BC/PU composites, it is expected that their surface could accomplish a reduced roughness compared with the surface of pristine dried BC membrane. To confirm our hypothesis, we performed an AFM analysis of the BC/PU composites and the pristine BC membrane. A low surface

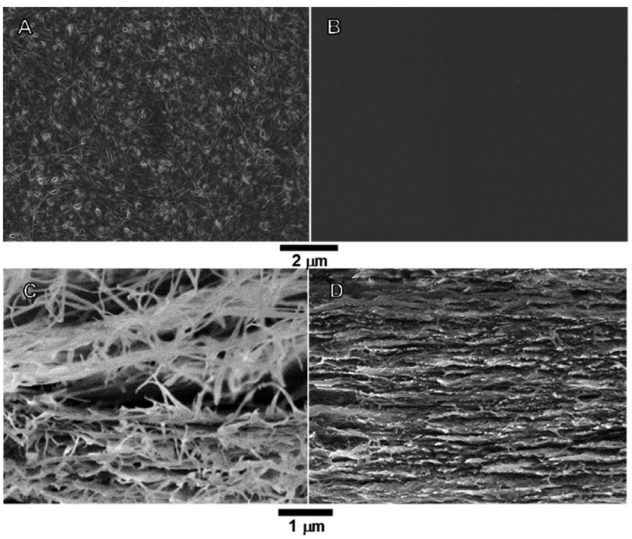

Fig. 2 SEM images of (A) the surface of the pristine dried BC membrane and (B) the surface of the BC/PU composite resulting from the solvent exchange process within 72 h. (C) Cross-section of the pristine dried BC membrane and (D) cross-section of the BC/PU composite resulting from the solvent exchange process within 72 h.

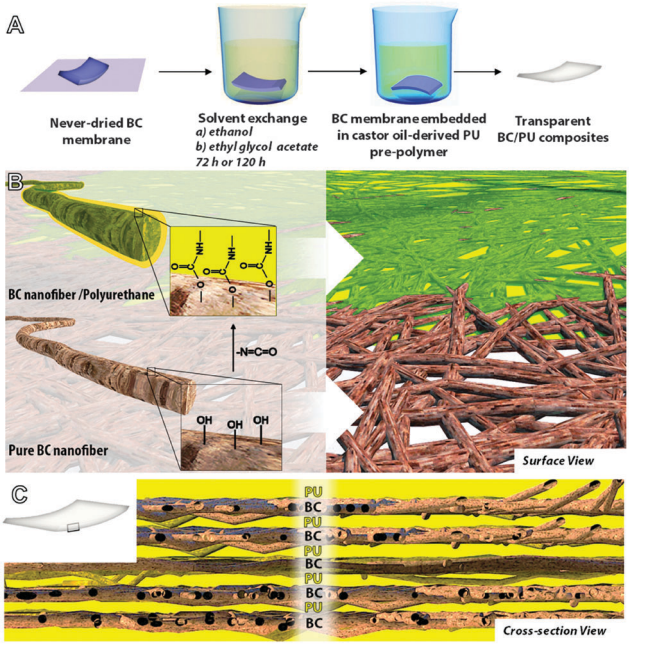

Fig. 3 Schematic illustration of (A) the protocol for the fabrication of BC/PU composites *via* a solvent exchange process, and (B) the surface view of the interface of the BC nanofibers naturally rich in hydroxyl bonds, and the post-modification with PU prepolymer through the formation of urethane bonds. (C) Cross-section view of the BC/PU composite, suggesting the formation of alternating layers of BC nanofibers filled with PU.

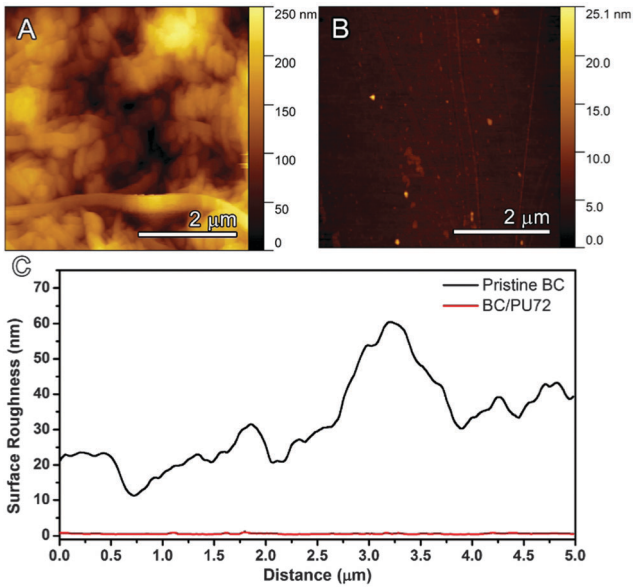

Fig. 4 Top view and 3D view of AFM images from (A) the pristine BC membrane and (B) the BC/PU composite resulted from the solvent exchange process within 72 h. (C) Graph of the surface roughness as a function of the distance for the pristine BC membrane and BC/PU composite extracted from tapping mode atomic force microscopy. When the BC nanofibers were covered with PU resin, the surface roughness greatly reduced from 32 ± 12.23 nm to 0.503 ± 0.1186 nm.

roughness is an important requirement for substrates based on polymers and should be kept lower than 5 nm[34] in the fabrication of suitable substrates for flexible OLEDs. Fig. 4A and B illustrate the top view of the AFM images evaluated in contact mode for the pristine BC membrane and BC/PU72 composite over an area of 25 μm^2. Fig. 4C shows a plot of surface roughness (Ra) as a function of distance for the pristine BC membrane and BC/PU72 composite. The Ra for pristine BC was about 32 nm and it is obviously associated with the noticeable coarse surface of the 3D network of BC nanofibers. On the other hand, the Ra determined for the BC/PU72 composite was 0.5 nm, a value 98% lower compared to the pristine BC membrane. This result confirms that the covering of the BC fibrils with PU was also very effective in affording a very smooth surface. Manuspiya *et al.*[35] reported the fabrication of composites from BC and commercial PU resin where the surface roughness was 81.39 nm. The authors also achieved a reduced roughness of 25.66 nm by polishing the surface of the composites.[36] To the best of our knowledge, our results demonstrate the smallest roughness value reported in the literature for BC/PU composites and even better than the ones subjected to surface post-treatment.

Fig. 5 shows the XRD patterns for the pristine BC membranes, pure PU resin film, and BC/PU composites. The XRD pattern of the pure PU resin film shown in Fig. 5a displays a single diffuse peak at 21° in 2θ, predominantly associated with the amorphous nature of the polymer. On the other hand, the nanofibers synthesized from bacteria contain a large amount of highly crystalline cellulose polymer and are free of amorphous phases such as lignin and hemicellulose abundantly present in plant-derived cellulose.

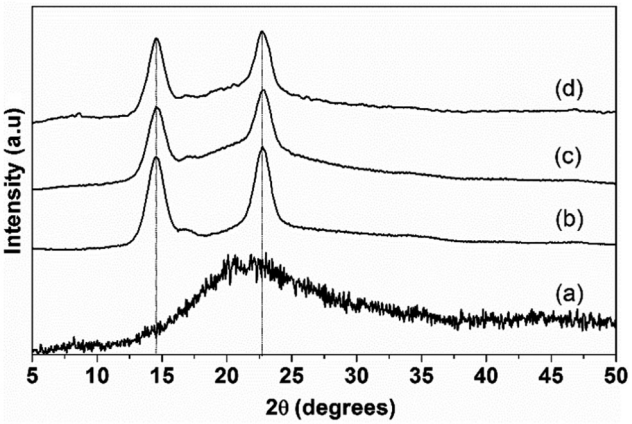

Fig. 5 X-Ray diffraction patterns of (a) the pure polyurethane film; (b) the pristine dried BC membrane and BC/PU composites resulted from the solvent exchange process within (c) 72 h and (d) 120 h.

As a result, the dried BC membrane is basically constituted of a semi-crystalline polymer, whose XRD pattern displays two broad reflection peaks localized at 15° and 22.5°, assigned to the 1α and 1β phases of native cellulose (*i.e.* type I cellulose) and overlapped by amorphous haloes.[37]

The peak at 15° is related to the contribution of the reflections from the monoclinic (110) and triclinic (100) planes. The peak at 22.5° corresponds to the contribution of the reflections from the monoclinic (002) and triclinic (110) planes.[37] Nevertheless, the BC/PU composites show similar diffraction pattern profiles compared to the pristine BC membrane, suggesting that a semi-crystalline structure is preserved during the experimental procedure. For clarity, we investigated the influence of the impregnation of PU in the cellulose by means of the calculus of the crystallinity of the BC membranes and BC/PU composites. To this end, we applied the Segal equation[38] (eqn (1)) to the extracted data from the XRD diffraction:

$$\mathrm{CrI} = \frac{I_{002} - I_{100}}{I_{002}} \times 100 \quad (1)$$

where CrI corresponds the relative degree of crystallinity, I_{002} is the maximum intensity of the (002) plane diffraction and I_{am} is the intensity of the amorphous halo at 2θ = 18°. According to the Segal equation, the pristine BC membrane shows a CrI value equal to 70%.[38] However, a slight decrease in crystallinity is observed after the impregnation of PU resin resulting in a CrI value of 64% for all BC/PU composites. We propose that the PU resin could penetrate into the cellulose chains and promote the breakdown of inter-chain hydroxyl hydrogen bonds, thereby causing the decrease of BC crystallinity.[39]

The thermal stability of pure BC, the PU film and BC/PU composites was evaluated using thermogravimetric analysis (not shown here). Although the BC/PU composite showed a higher thermal stability (248 °C for BC/PU72 and 266.5 °C for BC/PU120) compared to the pure PU film (233 °C), they display a thermal stability substantially lower than the pristine BC membrane (300 °C). The increase in the thermal degradation temperature of the BC/PU composites compared to the pure PU

film could be attributed to the strong interface of the PU prepolymer with the BC nanofibers, generating the previously mentioned cross-linked network obtained during the cure process with moisture and air.

Besides high transparency, thermal stability and low surface roughness, a highly desired substrate for the flexible OLED market, for example, should present obvious remarkable mechanical properties. Lately, the world's leading glass manufacturers have unveiled great efforts to introduce glass-based flexible substrates for OLED displays and lighting. For example, Corning® have developed an ultra-thin substrate (50 μm) known as Willow glass™ commercially considered as a potential alternative as a substrate for flexible OLED devices. Although it shows exceptional flexibility, it has been reported that such a glassy substrate exhibited shattering issues when the edges are stressed.[40] The BC/PU composites proposed in this work are thinner than the glass-based substrates and can reversibly bend into acute angles even when stressed on the edges. A more detailed investigation of the mechanical properties of the BC/PU composites was conducted by dynamic mechanical analysis using strips of cut samples. The tensile stress at break and the Young's modulus of the BC/PU composites were compared with the pristine BC membranes and pure PU film as summarized in Table 2.

Pure PU film is basically majority composed of castor oil based polyurethane polyether or polyester soft segments and by diisocyanate-based hard segments. Evidently, these features are greatly pronounced in the low tensile stress and Young's modulus of the PU pure films compared to the BC/PU composites. Additionally, the PU film displayed a significant deformation with a tensile strain of 24.5 MPa. The increase of both tensile stress at break and Young's modulus were consistent with the increase of cellulose content in the composites. In fact, the BC/PU composites loaded with a high content of cellulose outperform enhancements with a tensile strength of up to 69 MPa and a Young's modulus up to 6 GPa presumably because of the outstanding mechanical properties of individual BC nanofibers.

Remarkably, the facile combination of two special materials derived from renewable sources, namely castor oil based polyurethane and BC membranes, leads to flexible and transparent composites. Although transparent substrates based on cellulosic resins are abundantly reported in the literature, there are still few successful reports of their application in flexible electronics. The BC/PU composites were evaluated as compatible substrates for the fabrication of flexible OLEDs.

The OLED substrates were prepared by the deposition of a conductive thin film of ITO onto the surface of the BC/PU membrane and glass substrate. The electrical characteristic of both samples are detailed in Table 3. As can be seen, the ITO electrical characteristics measured for the BC/PU surface were similar to that of ITO on glass. This result also confirms a superior result when compared with the pristine BC based flexible OLEDs published in a previous report.[5] Despite the excellent surface roughness found in BC/PU composites, the resistivity of the ITO layer is slightly larger for the composites than the flat glass substrates. We conceive that the deviation of resistivity value might be attributed to the flexible feature of the BC/PU substrate. Both the flexible OLED and OLED presented a standard diode current density as a function of the applied voltage curve, as shown in Fig. 6. Furthermore, when compared

Table 2 Mechanical properties of the BC/PU composites compared to pristine BC membranes and pure PU film

	Stress (MPa)	Strain (%)	Young's module (GPa)
Pristine BC	179.9	2.6	13
BC/PU72	69.5	1.9	6.0
BC/PU120	65.8	2.1	4.7
Pure PU film	2.3	24.5	0.016

Table 3 Electrical characterization of an indium-tin-oxide thin film deposited onto the surface of a BC/PU composite resulted from the exchange solvent process within 72 h and a flat glass substrate

	Carrier number ($\times 10^{20}$ cm^{-3})	Carrier mobility (cm^2 V^{-1} s^{-1})	Resistivity ($\times 10^{-4}$ Ω cm)
BC/PU72	−5.17	20.89	5.78
Glass	−9.55	19.89	3.29

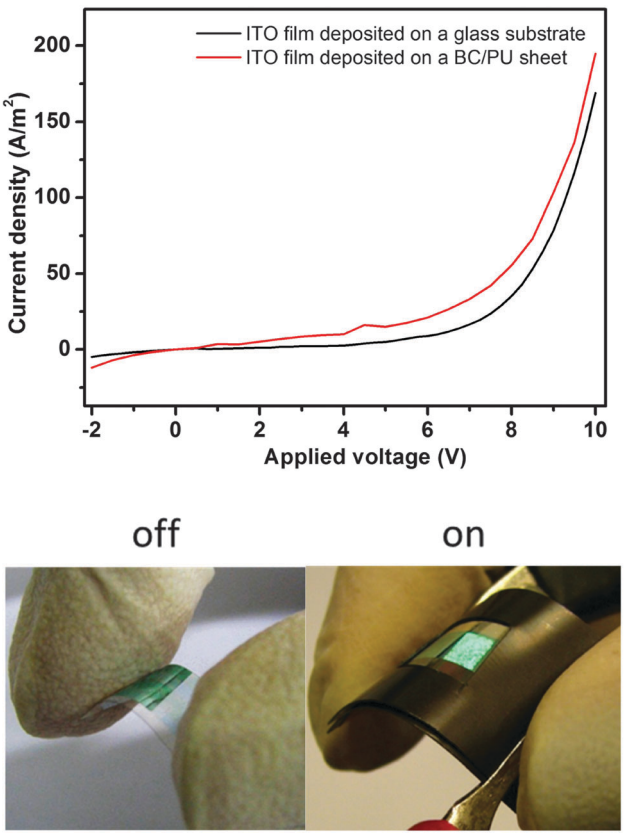

Fig. 6 Plot of the current density *versus* the applied voltage curves for the BC/PU composite resulted from the exchange solvent process within 72 h and the flat glass substrate, both coated with an indium-tin-oxide layer. The bottom section shows digital images of the working flexible OLEDs on the BC/PU composite when switched between "on" and "off" states. Black paper was placed around the transparent BC/PU to highlight the greenish brightness of the deposited electroluminescent layer when the substrate is switched to the "on" state.

with the glass substrate, the BC/PU flexible OLED displayed improved electrical performance since a higher current density with a lower applied voltage was achieved when compared with the flat glass substrate.

We investigated the luminance of the flexible OLED and OLED for both BC/PU and the glass substrates by applying the same current density and tension through the device, about 20 A m^{-2} and 10 V. The measurements were performed in triplicate and the luminance results of the flexible OLED were 231 $\pm$18 cd m^{-2} for BC/PU and 485 $\pm$ 8 cd m^{-2} for the flat glass substrate. It should be noted that technical difficulties were encountered when measuring the luminance of the flexible OLED due to the occurrence of folds during the acquisition. This might have negatively influenced the flexible OLED luminance result. Additionally, Fig. 6 shows the digital images of a transparent flexible OLED built on the BC/PU composites switched between on/off states.

A high quality ITO deposition was accomplished onto free-standing films of the BC/PU composite. Because of the high transparency (>90%) and flexibility, we suggest that BC/PU composites are potential candidates for substrates of flexible electronic display devices.

Conclusions

Flexible and transparent freestanding films of bacterial cellulose (BC) and castor oil based polyurethane (PU) prepolymer were fabricated using an easy solvent exchange protocol. The BC/PU composites comprise thin free-standing films (<50 μm) displaying high transparency in the ultraviolet (up to 70% at 350 nm) and visible regions (up to 90% at 700 nm) besides low surface roughness (<1 nm) which are fundamental requisites of substrates for lighting-emitting devices and displays. Additionally, the BC/PU composites were semi-crystalline and displayed good thermal stability (>250 °C). In fact, the introduction of polyurethane endows exceptional improvements of the optical properties of BC membranes while the addition of BC nanofibers delivers the fabrication of films with higher breaking strength. The accomplishment of flexible and transparent composites is due to the unique interface between the BC nanofiber surface and PU prepolymer. It is important to note that the uniformity of distribution of PU throughout the 3D network of BC nanofibers was remarkably achieved only *via* an exchange solvent process rather than other methods (*e.g.* hot pressed and UV-curing methods) used in the literature. The BC/PU composite features offer exciting new opportunities as substrates for flexible electronic displays. Besides, it must be considered that the bacterial cellulose and castor oil were obtained from renewable resources and can potentially be subjected to conventional decomposition by microorganisms in soil, along with the degradation production of H_2O, CO_2, and aromatic ethers.

Acknowledgements

Financial support from Brazilian agencies: State of São Paulo Research Foundation (FAPESP), Coordination for the Improvement of Higher Education Personnel (CAPES) and National Council for Scientific and Technological Development (CNPq) and technical support of Electron Microscopy Laboratory (LME, Araraquara, BR) are acknowledged.

References

1 D. Klemm, F. Kramer, S. Moritz, T. Lindstrom, M. Ankerfors, D. Gray and A. Dorris, *Angew. Chem.*, 2011, **50**, 5438–5466.
2 G. Guhados, W. Wan and J. L. Hutter, *Langmuir*, 2005, **21**, 6642–6646.
3 A. Nakagaito and H. Takagi, in *Handbook of Polymer Nanocomposites. Processing, Performance and Application*, ed. J. K. Pandey, H. Takagi, A. N. Nakagaito and H.-J. Kim, Springer, Berlin Heidelberg, 2015, ch. 68, pp. 343–353.
4 B. Geffroy, P. Le Roy and C. Prat, *Polym. Int.*, 2006, **55**, 572–582.
5 C. Legnani, C. Vilani, V. L. Calil, H. S. Barud, W. G. Quirino, C. A. Achete, S. J. L. Ribeiro and M. Cremona, *Thin Solid Films*, 2008, **517**, 1016–1020.
6 M. D. J. Auch, O. K. Soo, G. Ewald and C. Soo-Jin, *Thin Solid Films*, 2002, **417**, 47–50.
7 Y. Okahisa, A. Yoshida, S. Miyaguchi and H. Yano, *Compos. Sci. Technol.*, 2009, **69**, 1958–1961.
8 T. Nishino, I. Matsuda and K. Hirao, *Macromolecules*, 2004, **37**, 7683–7687.
9 M. Nogi and H. Yano, *Adv. Mater.*, 2008, **20**, 1849–1852.
10 S. C. M. Fernandes, L. Oliveira, C. S. R. Freire, A. J. D. Silvestre, C. Pascoal Neto, A. Gandini and J. Desbrieres, *Green Chem.*, 2009, **11**, 2023–2029.
11 H. S. Barud, J. L. Souza, D. B. Santos, M. S. Crespi, C. A. Ribeiro, Y. Messaddeq and S. J. L. Ribeiro, *Carbohydr. Polym.*, 2011, **83**, 1279–1284.
12 C. Tang and H. Liu, *Composites, Part A*, 2008, **39**, 1638–1643.
13 H. S. Barud, J. M. A. Caiut, J. Dexpert-Ghys, Y. Messaddeq and S. J. L. Ribeiro, *Composites, Part A*, 2012, **43**, 973–977.
14 Y. Kim, R. Jung, H. S. Kim and H. J. Jin, *Curr. Appl. Phys.*, 2009, **9**, S69–S71.
15 H. Yano, J. Sugiyama, A. N. Nakagaito, M. Nogi, T. Matsuura, M. Hikita and K. Handa, *Adv. Mater.*, 2005, **17**, 153–155.
16 C. K. Williams and M. A. Hillmyer, *Polym. Rev.*, 2008, **48**, 1–10.
17 A. Zlatanić, C. Lava, W. Zhang and Z. S. Petrović, *J. Polym. Sci., Part B: Polym. Phys.*, 2004, **42**, 809–819.
18 V. D. Athawale and P. S. Pillay, *J. Polym. Mater.*, 2003, **20**, 317–326.
19 H. Mutlu and M. A. R. Meier, *Eur. J. Lipid Sci. Technol.*, 2010, **112**, 10–30.
20 H. J. Wang, M. Z. Rong, M. Q. Zhang, J. Hu, H. W. Chen and T. Czigany, *Biomacromolecules*, 2008, **9**, 615–623.
21 C. Zhang, H. Wu and M. R. Kessler, *Polymer*, 2015, **69**, 52–57.
22 V. R. Botaro, A. Gandini and M. N. Belgacem, *J. Thermoplast. Compos. Mater.*, 2005, **18**, 107–117.

23 D. Klemm, D. Schumann, F. Kramer, N. Hessler, M. Hornung, H. P. Schmauder and S. Marsch, *Polysaccharides*, 2006, **205**, 49–96.
24 P. Chen, S. Y. Cho and H. J. Jin, *Macromol. Res.*, 2010, **18**, 309–320.
25 S. J. Eichhorn, A. Dufresne, M. Aranguren, N. E. Marcovich, J. R. Capadona, S. J. Rowan, C. Weder, W. Thielemans, M. Roman, S. Renneckar, W. Gindl, S. Veigel, J. Keckes, H. Yano, K. Abe, M. Nogi, A. N. Nakagaito, A. Mangalam, J. Simonsen, A. S. Benight, A. Bismarck, L. A. Berglund and T. Peijs, *J. Mater. Sci.*, 2010, **45**, 1–33.
26 J. Juntaro, S. Ummartyotin, M. Sain and H. Manuspiya, *Carbohydr. Polym.*, 2012, **87**, 2464–2469.
27 S. Ummartyotin, J. Juntaro, M. Sain and H. Manuspiya, *Ind. Crops Prod.*, 2012, **35**, 92–97.
28 K. D. Vorlop, A. Muscat and J. Beyersdorf, *Biotechnol. Tech.*, 1992, **6**, 483–488.
29 I. M. Arcana, B. Bundjali, M. Hasan, K. Hariyawati, H. Mariani, S. D. Anggraini and A. Ardana, *J. Polym. Environ.*, 2010, **18**, 188–195.
30 E. De Carlo, Master degree dissertation, University of São Paulo, 2002.
31 J. Ganster and H.-P. Fink, in *Handbook of Polymers*, ed. J. Brandrup, E. H. Immergut and E. A. Grulke, John Wiley & Sons, New York, 4th edn, 1999, ch. V, pp. 135–152.
32 A. N. Nakagaito, M. Nogi and H. Yano, *MRS Bull.*, 2010, **35**, 214–218.
33 J. Juntaro, M. Pommet, A. Mantalaris, M. Shaffer and A. Bismarck, *Compos. Interfaces*, 2007, **14**, 753–762.
34 M.-C. Choi, Y. Kim and C.-S. Ha, *Prog. Polym. Sci.*, 2008, **33**, 581–630.
35 S. Ummartyotin, J. Juntaro, M. Sain and H. Manuspiya, *Carbohydr. Polym.*, 2011, **86**, 337–342.
36 S. Ummartyotin, J. Juntaro, M. Sain and H. Manuspiya, *Chem. Eng. J.*, 2012, **193**, 16–20.
37 M. Wada, J. Sugiyama and T. Okano, *J. Appl. Polym. Sci.*, 1993, **49**, 1491–1496.
38 L. Segal, J. J. Creely, A. E. Jr Martin and C. M. Conrad, *Text. Res. J.*, 1959, **29**, 786–794.
39 D. T. B. De Salvi, H. S. Barud, J. M. A. Caiut, Y. Messaddeq and S. J. L. Ribeiro, *J. Sol-Gel Sci. Technol.*, 2012, **63**, 211–218.
40 G. Mone, *Commun. ACM*, 2013, **56**, 16–17.

